HHS Public Access

Author manuscript

Nat Microbiol. Author manuscript; available in PMC 2017 October 31.

Published in final edited form as:

Nat Microbiol. ; 1(9): 16133. doi:10.1038/nmicrobiol.2016.133.

Suppression of autophagy and antigen presentation by *Mycobacterium tuberculosis* PE_PGRS47

Neeraj K. Saini[1,†], **Andres Baena**[1,†,‡], **Tony W. Ng**[1], **Manjunatha M. Venkataswamy**[1,‡], **Steven C. Kennedy**[1], **Shajo Kunnath-Velayudhan**[1], **Leandro J. Carreño**[1,‡], **Jiayong Xu**[2], **John Chan**[2], **Michelle H. Larsen**[1,3], **William R. Jacobs Jr**[1,3], and **Steven A. Porcelli**[1,2,*]

[1]Department of Microbiology and Immunology, Albert Einstein College of Medicine, Bronx, New York 10461, USA

[2]Department of Medicine, Albert Einstein College of Medicine, Bronx, New York 10461, USA

[3]Howard Hughes Medical Institute, Albert Einstein College of Medicine, Bronx, New York 10461, USA

Abstract

Suppression of major histocompatibility complex (MHC) class II antigen presentation is believed to be among the major mechanisms used by *Mycobacterium tuberculosis* to escape protective host immune responses. Through a genome-wide screen for the genetic loci of *M. tuberculosis* that inhibit MHC class II-restricted antigen presentation by mycobacteria-infected dendritic cells, we identified the PE_PGRS47 protein as one of the responsible factors. Targeted disruption of the *PE_PGRS47* (*Rv2741*) gene led to attenuated growth of *M. tuberculosis in vitro* and *in vivo*, and a *PE_PGRS47* mutant showed enhanced MHC class II-restricted antigen presentation during *in vivo* infection of mice. Analysis of the effects of deletion or over-expression of PE_PGRS47 implicated this protein in the inhibition of autophagy in infected host phagocytes. Our findings identify PE_PGRS47 as a functionally relevant, non-redundant bacterial factor in the modulation of innate and adaptive immunity by *M. tuberculosis*, suggesting strategies for improving antigen presentation and the generation of protective immunity during vaccination or infection.

Mycobacterium tuberculosis (Mtb) persists within mammalian hosts through a variety of immune evasion strategies, including the inhibition of multiple antigen presentation

*Correspondence and requests for materials should be addressed to S.A.P.: steven.porcelli@einstein.yu.edu.
†These authors contributed equally to this work.
‡Present addresses: Grupo de Inmunología Celular e Inmunogenética (GICIG), Departamento de Microbiología y Parasitología, Facultad de Medicina, Universidad de Antioquia, Calle 70 No. 52-21, Medellín, Colombia (A.B.); Department of Neurovirology, NIMHANS, 560029 Bangalore, India (M.M.V.); Millenium Institute on Immunology and Immunotherapy, Programa Disciplinario de Inmunologia, Universidad de Chile, Chile (L.J.C.).

Author contributions

N.K.S., A.B. and T.W.N. designed and carried out experiments. S.A.P. supervised the design and execution of all experiments. M.M.V., S.C.K., S.K.-V., L.J.C. and J.X. assisted in the execution of selected experiments. J.C., M.H.L. and W.R.J. provided input on the design of experiments and data interpretation. All authors contributed to writing and editing the manuscript.

Additional information

Supplementary information is available online. Reprints and permissions information is available online at www.nature.com/reprints.

Competing interests

The authors declare no competing financial interests.

pathways that are central to adaptive immunity[1]. Major histocompatibility complex (MHC) class II molecules, which control $CD4^+$ T-cell responses, are critical for host resistance to Mtb, and the bacilli have evolved the ability to modulate the expression and function of these molecules[2–8]. Autophagy is a ubiquitous cellular process that participates in the processing of antigens for MHC class II antigen presentation[9–12], and in cells infected by vacuolar pathogens like Mtb it provides a potential mechanism to initiate phagosome maturation and enhance the processing and presentation of their antigens to T cells[12–14]. Recent evidence suggests that Mtb has developed immune evasion strategies that interfere with autophagy, thus improving its intracellular survival and limiting the presentation of its antigens by MHC class II. Although several mycobacterial factors have been implicated in this aspect of immune evasion[15–17], the mechanisms and specific mediators involved remain mostly unknown.

In the current study, we undertook a genome-wide gain of function screen to identify genes of Mtb involved in the inhibition of MHC class II presentation in Mtb-infected cells. This identified at least five genomic loci of Mtb that independently contribute to the inhibition of MHC class II-restricted antigen presentation, several of which also blocked autophagy. Detailed analysis of one of these loci implicated *PE_PGRS47*, a member of a large family of virulence-related genes in Mtb, as an inhibitor of autophagy and a factor contributing to evasion of both innate and adaptive immunity by Mtb. These findings identify a specific mycobacterial factor involved in the evasion of innate and adaptive immunity against Mtb and provide new insight into the role of PE_PGRS proteins in tuberculosis.

Results

Isolation of Mtb genes that inhibit MHC class II presentation

A cosmid library of random Mtb genomic DNA fragments (~20–35 kilobases) was used to transform the nonpathogenic mycobacterium *M. smegmatis* (Msmeg), and several hundred individual clones were screened for their ability to impair MHC class II presentation of bacterial antigens by bone marrow-derived dendritic cells (BMDCs). We used Msmeg expressing an Mtb ESAT-6 protein extended at its C terminus to include a well-characterized MHC class II presented epitope (I-E$\alpha_{52–68}$) for this screening, which allowed direct measurement of antigen presentation using monoclonal antibody Y-Ae, specific for complexes of I-E$\alpha_{52–68}$ bound to MHC class II (I-A^b) molecules[18] (Supplementary Fig. 1). From a total of 365 Msmeg transformants harbouring random Mtb genomic cosmids, five were identified that gave a significant and reproducible reduction of cell surface Y-Ae staining while maintaining the expression of the ESAT6-IEα fusion protein (Fig. 1a and Supplementary Fig. 2). Restriction mapping of re-extracted cosmid DNA revealed that each cosmid contained distinct and non-overlapping inserts of Mtb genomic DNA (Supplementary Fig. 2). None of these Msmeg clones affected the level of total cell surface MHC class II expression on infected BMDCs (Fig. 1b). This indicated that the reduced antigen presentation was not due to global down-regulation of MHC class II expression, which has been previously attributed to Mtb (ref. 5). The reduction in cell surface expression of MHC class II/peptide complexes was also confirmed in assays of T-cell responses using $CD4^+$ T cells specific for I-A^b/E$\alpha_{52–68}$ peptide complexes (Fig. 1c). Taken together, our

results indicate at least five genomic loci in Mtb encoding the potential to inhibit the processing or presentation of bacteria-derived MHC class II presented antigens.

Effects of Mtb genes on autophagy

The inhibition of antigen presentation by Mtb genes without reduction in total surface MHC class II suggested effects on the digestion of intra-phagosomal bacteria and reduced delivery of their antigens to endocytic compartments containing MHC class II molecules. Consistent with this, we observed that three of the five Msmeg transformants inhibiting antigen presentation showed a significant increase in persistence of viable bacteria at 24 h following *in vitro* infection of BMDCs (Fig. 1d). These findings suggested an effect on autophagy, a basic cellular process that restricts the survival of intracellular mycobacteria[13,14,19] and also promotes intracellular antigen processing for MHC class II presentation[20]. To examine this, we assessed the distribution of microtubule-associated light chain 3 (LC3), a central component of autophagosome formation that undergoes cleavage, lipid modification and cellular redistribution during autophagosome formation[21]. Initial experiments showed that infection of a macrophage cell line with wild-type Msmeg triggered the formation of LC3 punctate structures in the cytoplasm, which were visualized by staining with an anti-LC3 mAb. In contrast, infections with Msmeg transformed with cosmid M2D10, M2H6 or S1G7 were associated with a significant reduction of the LC3 puncta formation as compared with cells infected with control Msmeg harbouring empty cosmid (pYUB412; Fig. 1e,f). Similar results were obtained using an LC3–GFP reporter fusion protein (Supplementary Fig. 3a,b). Biochemical analysis of LC3 protein also confirmed an effect on autophagy, showing that the increase in the LC3-II/LC3-I ratio was substantially reduced (25–85%) in cells infected with bacteria harbouring the same cosmids that reduced LC3 puncta formation (Supplementary Fig. 3c).

Identification of *PE_PGRS47* as an autophagy-inhibiting Mtb gene

As a first step towards the identification of specific Mtb genes responsible for the inhibition of autophagy and antigen presentation, we focused on cosmid M2D10 and generated a complete map of open reading frames (ORFs) from the sequence of its ~35 kb insert (Supplementary Fig. 4). Based on annotation of the Mtb genome and published literature, one gene among the 33 intact ORFs stood out as a candidate for direct involvement in host–pathogen interactions. This was *PE_PGRS47* (*Rv2741*), a member of the large family of *PE_PGRS* genes implicated in pathogenesis and intracellular survival of virulent mycobacteria (Supplementary Fig. 5)[22,23]. Initial experiments showed that expression of PE_PGRS47 in Msmeg phenocopied the inhibition of autophagy in infected macrophages observed with Msmeg transformed with cosmid M2D10, and also demonstrated that PE_PGRS47 was secreted by the bacteria and could gain access to the cytosol of infected phagocytic cells (Supplementary Fig. 6). We thus proceeded to directly explore the role of *PE_PGRS47* in Mtb infection by constructing a precise deletion mutant in the virulent Mtb H37Rv strain using specialized phage transduction (Supplementary Fig. 7a–d)[24]. In addition, a complemented strain was generated by reintroducing *PE_PGRS47* into the Δ*PE_PGRS47* mutant. The Δ*PE_PGRS47* and complemented strains showed identical growth in standard liquid medium as wild-type Mtb, and similar growth *in vivo* in the lungs

during the first four weeks following low-dose aerosol infection of C57BL/6 mice (Supplementary Fig. 7e,f).

To assess the role of *PE_PGRS47* in blocking autophagy during Mtb infection, mouse macrophage cell line RAW264.7 was infected with wild-type, mutant or complemented strains and examined for LC3 punctate structures by fluorescence microscopy. This revealed an increase in LC3 puncta with infection by the mutant (Fig. 2a,b). Following infection of RAW264.7 cells with the Δ*PE_PGRS47* mutant we also observed an increase in conversion of LC3-I to LC3-II compared to cells infected with wild-type or complemented strains (Fig. 2c). We also examined effects on the levels of p62 (sequestosome 1), which is recruited to newly formed autophago-somes and subsequently degraded[25]. We observed a greater level of p62 in cells infected with wild-type Mtb than Δ*PE_PGRS47* mutant infection, which was reversed by complementation (Fig. 2d). Furthermore, using wild-type, Δ*PE_PGRS47* and complemented strains of Mtb expressing TdTomato, an increase in the co-localization of intracellular bacteria with LC3 punctate structures was shown for the Δ*PE_PGRS47* mutant in infected RAW264.7 cells (Fig. 2e,f). Transmission electron microscopy of cells infected with the mutant showed bacilli within the characteristic double-membrane autophagosomes associated with the initial stages of engulfment by autophagy; such structures were not observed in cells infected with wild-type Mtb (Fig. 2g). Altogether, these results indicate a significant role for *PE_PGRS47* in preventing the formation or a detectable level of accumulation of autophagosomes containing intracellular Mtb.

Effects of *PE_PGRS47* on maturation of mycobacterial phagosomes

The engulfment of mycobacteria within autophagosomes can lead to further maturation of these compartments, including acidification and fusion with lysosomes. We thus carried out studies to assess the role of *PE_PGRS47* in blocking mycobacterial phagosome acidification and phagolysosomal fusion. RAW264.7 cells were labelled with LysoTracker dye, which labels acidic late endosomes and lysosomes, and then infected with wild-type, Δ*PE_PGRS47* or complemented strains of Mtb. This revealed a significant increase in co-localization with the mutant compared to wild-type Mtb, which was reversed by complementation (Fig. 3a,b). We also observed a significant increase in co-localization between the Δ*PE_PGRS47* mutant and the lysosomal marker lysosome-associated membrane protein 1 (LAMP-1) (Fig. 3a,b), indicating enhanced lysosomal fusion with infected phagosomes.

Role of PE_PGRS47 during chronic Mtb infection

Whereas initial findings showed that deletion of *PE_PGRS47* had no effect on the growth of Mtb in mice early after infection (Supplementary Fig. 7f), subsequent analysis of colony-forming unit (c.f.u.) levels from tissues of wild-type mice at 15 or 25 weeks post-infection showed that the Δ*PE_PGRS47* strain was significantly attenuated in chronic stages of disease (Fig. 4a). Histological examination of the lungs at 15 weeks post-infection showed reductions in leukocyte accumulation and in the total area of histologically infiamed lung tissue in animals infected with the mutant compared to wild-type or complemented strains (Fig. 4b). To examine this in the absence of adaptive immunity, severe combined immunodeficient (SCID) mice were infected intravenously with a high dose (10^6 c.f.u.) of

Mtb mutant, wild-type and complemented strains, then followed for survival. This also showed that the Δ*PE_PGRS47* strain was significantly attenuated *in vivo* (Fig. 4c), indicating an increased susceptibility to innate immune mechanisms. Similarly, *in vitro* infection in RAW264.7, human THP-1 myelomonocytic cells and BMDCs showed that the mutant had very little capacity for intracellular growth, remaining at static levels based on sampling at various intervals during the five days of culture compared to the wild-type or complemented strains (Supplementary Fig. 8a). To confirm a role for autophagy in this reduced intracellular survival of Δ*PE_PGRS47*, we infected RAW264.7 cells or BMDCs with the Δ*PE_PGRS47*, wild-type Mtb and complemented strains in the presence or absence of 3-methyladenine (3MA), an inhibitor of autophagy. This showed that the reduced bacterial burden of the Δ*PE*_PGRS47 mutant could be fully restored to wild-type Mtb levels by the addition of 3MA (Fig. 4d). In contrast, no significant changes in c.f.u. levels were observed with 3MA treatment of cells infected with wild-type Mtb or complemented strains (Supplementary Fig. 8b). These results are consistent with an important role for the *PE_PGRS47* gene in the growth and survival of Mtb, particularly during intracellular growth and in the later chronic phase of infection.

Inhibition of MHC class II antigen presentation by PE_PGRS47

To assess the ability of PE_PGRS47 to suppress MHC class II dependent antigen presentation during Mtb infection, we carried out studies both *in vitro* and *in vivo*. Presentation to MHC class II-restricted T-cell hybridomas was assessed *in vitro* for BMDCs infected with the Δ*PE_PGRS47* mutant compared to wild-type or complemented strains. This showed enhanced responses for hybridomas specific for Mtb secreted antigens TB9.8 or antigen 85B (Ag85B). Treatment of the BMDCs with the autophagy inhibitor 3MA reduced the responses to both antigens and eliminated the increase associated with deletion of *PE_PGRS47*. Conversely, addition of rapamycin to activate autophagy gave increased T-cell responses, while also eliminating the enhanced responses to the Δ*PE_PGRS47* strain compared to wild-type or complemented strains (Fig. 5a). Overall, these results were consistent with an autophagy-dependent enhancement of MHC class II presentation with deletion of *PE_PGRS47*. To rule out the possibility that *PE_PGRS47* deletion could alter the total surface level of MHC class II on infected BMDCs, we analysed this by flow cytometry. This showed no significant effect of *PE_PGRS47* deletion on the total surface level of MHC class II expression in infected BMDCs compared to wild-type Mtb or complemented strains (Fig. 5b).

To assess MHC class II presentation *in vivo*, we infected C57BL/6 mice with wild-type, Δ*PE_PGRS47* or complemented Mtb strains and measured $CD4^+$ T-cell responses against well-defined Mtb antigens. Lungs, spleen and mediastinal lymph nodes (MLN) were collected on different days post-infection and processed to obtain single-cell suspensions. Using flow cytometry to quantitate cells binding an MHC class II ($I\text{-}A^b$) tetramer containing a peptide from the secreted antigen TB9.8 (EsxG), we detected significantly more TB9.8-specific $CD4^+$ T cells in all the organs of mice infected with the Δ*PE_PGRS47* mutant compared to mice infected with wild-type or complemented strains on day 24 post-infection (Fig. 6a). However, we were not able to detect effects on the frequency of TB9.8-specific $CD4^+$ T cells at very early phases of infection on days 9 or 14 (Supplementary Fig. 9),

suggesting that PE_PGRS47 is not active in the initial stages of infection and may not affect the initial priming of T cells.

We also performed interferon-γ (IFNγ) enzyme-linked immunospot (ELISPOT) on cells isolated from infected mice to quantitate responses to immunodominant I-A^b presented epitopes from Mtb antigens ESAT-6, TB9.8 and Antigen 85B (Ag85B P25) (Fig. 6b). This showed significant increases in IFNγ-secreting $CD4^+$ T cells specific for TB9.8 in all tissues studied on day 24 in Δ*PE_PGRS47*-mutant-infected mice, compared to mice infected with wild-type Mtb or the complemented strains. At this time point, we also detected a significant increase in the lungs of $CD4^+$ T cells specific for Ag85B P25, which is known to be highly expressed by Mtb as an immunodominant antigen during early infection[26]. Surprisingly, we were not able to detect any increase in the frequency of $CD4^+$ T cells specific for ESAT-6, possibly reflecting the rapid expression of this antigen in the early phase of infection when PE_PGRS47 may not be active, or alternatively due to the ability of ESAT-6 to directly lyse phagosomal membranes and gain access to other cellular compartments[27–29]. These effects on TB9.8 and Ag85 P25 responses persisted or became more prominent by day 60 post-infection. Together, these results indicate a significant role for *PE_PGRS47* in the inhibition of MHC class II mediated antigen presentation of a subset of immunodominant $CD4^+$ T-cell antigens beginning in early infection and persisting into the later chronic phase.

Discussion

We have provided evidence for at least five distinct genomic loci and the identity of one specific gene of Mtb that contribute to the inhibition of MHC class II restricted antigen presentation. Expression of several of these loci in Msmeg significantly prolonged intracellular survival of the bacteria, and three of them also suppressed autophagy in infected cells. Overall, these findings are consistent with the prevalent view of a highly complex programme of immune evasion that allows survival of Mtb despite an intact immune system[5]. Sequence analysis of the five cosmids isolated in our screening did not identify known virulence-related genes, but the presence of *Rv2741*, encoding a member of the expanded PE_PGRS protein family of Mtb, provided a strong candidate for a relevant immune evasion gene in one of the five cosmids (M2D10). Although the precise functions of PE_PGRS proteins or potential non-protein coding functions of *PE_PGRS* genes remain mostly unknown, previous studies have implicated members of this family in virulence and immune evasion by pathogenic mycobacteria[22,23].

Our studies focusing on *PE_PGRS47* showed that this gene significantly modulates intracellular infection. The Δ*PE_PGRS47* deletion mutant of Mtb showed a reduced capacity to inhibit autophagy and an increased acidification and lysosomal fusion of phagosomes during infection of phagocytic cells (Figs 2 and 3). In addition, infection of mice with the mutant revealed attenuated growth (Fig. 4) and a significant increase in $CD4^+$ T-cell responses against MHC class II presented antigens (Figs 5 and 6). These findings indicated a non-redundant role for PE_PGRS47 in modulating innate intracellular host responses, as well as in the generation of adaptive immune responses that are critical for control of Mtb. We have not yet carried out experiments using mouse strains with specific mutations in autophagy-related genes to further confirm and explore the effects of PE_PGRS47.

However, our current data using pharmacologic agents to manipulate this pathway (Figs 4d and 5a) support the hypothesis that PE_PGRS47 mediates linked inhibition of autophagy and antigen presentation in Mtb-infected cells. It is noteworthy that the expression of many PE_PGRS family members, including PE_PGRS47, is upregulated by mycobacteria after entering macrophages[30], and that PE_PGRS47 has been reported as one of the members of this family showing the highest level of evolutionary conservation[31].

Autophagy has received considerable attention as a basic cellular mechanism contributing to both innate and adaptive immunity[32], and as a mechanism that enhances clearance of intracellular myco-bacteria[33]. It has been frequently emphasized that Mtb inhibits phagosome maturation, preventing acidification of phagosomes harbouring live bacilli and their fusion with lysosomes[34]. Recent work suggests that this critical feature of Mtb survival and immune evasion is at least in part due to the suppression of auto-phagy[14,35,36]. Although a recent report has called into question the relevance of autophagy as a mechanism of host protection in the mouse model[37], this may reflect the ability of Mtb to efficiently disable and manipulate this pathway. Several of our findings were consistent with the expected effect of enhanced autophagy on promoting killing of Mtb by innate immunity (Fig. 4c and Supplementary Fig. 8a), but it was surprising that growth of the Δ*PE_PGRS47* mutant was not significantly attenuated in the early phase of infection in wild-type mice (Fig. 4a and Supplementary Fig. 7f). This suggests that other mediators may be produced by Mtb that play a more dominant role during the early phases of infection *in vivo* to prevent autophagy or to neutralize its microbicidal effects.

Overall, our results identify the product of the *PE_PGRS47* gene as one potentially important factor contributing to the modulation of the host cell environment by Mtb. The mechanism by which *PE_PGRS47* mediates this function remains to be determined, although our results indicate that this protein is secreted by the bacteria and gains access to the cytosol of infected host cells (Supplementary Fig. 6). Access to the host cell cytoplasm has been described for other PE_PGRS proteins, such as PE_PGRS33, which has been reported to localize to mitochondria to modulate cell death[38]. Specific interacting partners for PE_PGRS proteins within the host-cell proteome have not yet been identified, and this represents an important future area of discovery that may yield clues to the mechanisms of action of PE_PGRS47 and other members of this family.

Methods

Antibodies and other reagents

Monoclonal antibody Y-Ae was purified from hybridoma culture supernatants by standard protein G column chromatography (Amersham Biosciences/GE Healthcare). Purified mAbs (2.0 mg ml^{-1} in PBS) were biotinylated overnight at 4 °C using NHS–LC–biotin (N-Hexanoate-succinimidyl-long chain-biotin, Thermo scientific), dissolved to 10 mM with DMSO just before use, with a biotin-to-mAb molar ratio of 30:1. Unbound biotin was not removed, as this did not interfere with downstream applications. Anti-I-A/I-E-FITC (fluorescein isothiocyanate) and anti-CD11c-PE mAbs were obtained from BD Biosciences. Rapamycin was from Calbiochem and IFNγ was from Peprotech. 3-Methyladenine was from Sigma. The nuclear fluorescent dye 4,6-diamidino-2-phenylindole (DAPI) was

purchased from Sigma. Anti-LC3 antibodies for western blotting and immunofluorescence analysis were purchased from Novus Biologicals and Cell Signaling, respectively. Antibodies to LAMP-1, β-actin and p62 were purchased from Abcam.

Bacterial strains and culture conditions

Wild-type Mtb (strain H37Rv), mutant and complemented strains or Msmeg (strain *mc*^{2}*155*) were cultured at 37 °C in Middlebrook 7H9 broth, or on 7H10 or 7H11 agar containing 10% (vol/vol) oleic acid–albumin–dextrose–catalase (OADC), 0.5% glycerol and 0.05% (vol/vol) tyloxapol. *Escherichia coli* strain DH5α was used for cloning purposes and grown on Luria–Bertani agar or broth at 37 °C. Strains bearing antibiotic resistance cassettes were cultured in the presence of hygromycin (50 μg ml^{-1} for mycobacterial selection or 150 μg ml^{-1} for *E. coli*) or kanamycin (20 μg ml^{-1} for mycobacterial selection or 40 μg ml^{-1} for *E. coli*). Strains of Msmeg and Mtb were transformed using published protocols[39]. The *PE_PGRS47* gene was deleted from Mtb H37Rv by allelic exchange via the previously described specialized phage transduction method[24]. Colonies were selected for hygromycin resistance following transduction, screened for gene deletion by PCR and confirmed by Southern blotting using previously described methods[24]. For complementation of the Δ*PE_PGRS47* mutant, a full-length Mtb *PE_PGRS47* (*Rv2741*) gene was amplified by PCR from Mtb H37Rv genomic DNA and cloned into pMV361, an integrating Mtb vector with an *hsp60* promoter[40].

Construction of Mtb genomic DNA library

The strategy for generation of the Mtb genomic library in cosmid vector pYUB412 has been described previously[47]. Briefly, *M. tuberculosis* (strain H37Rv) genomic DNA was purified and partially digested with Sau3A. Agarose gel purification was used to enrich for DNA fragments of ~40 kb, which were ligated into the arms of cosmid vector pYUB412 digested with BamH1. DNA was packaged into phages *in vitro* with Gigapack XL (Stratagene) and *E. coli* were transduced and selected on LB plates containing 100 μg ml^{-1} ampicillin. Over 1 × 10^5 independent clones were pooled, and DNA for transformation was obtained using standard alkaline lysis method.

Construction and expression of ESAT6-IEα fusion protein

A sequence of 87 bp containing the coding sequence for the MHC class II-presented IEα epitope (EFAKFASFEAQGALANIAVDKANLD)[48] was synthesized (GenScript) and then ligated into pMV261 containing the ESAT6 sequence to create a fusion of the IEα sequence to the C-terminal sequence of ESAT6. The resulting plasmid, pMV261-ESAT6-IEα, was introduced into *M. smegmatis* by electroporation.

Construction and screening of *M. smegmatis* clones expressing Mtb cosmids

The Mtb cosmid DNA library was electroporated into *M. smegmatis* harbouring the pMV261-ESAT6-IEα plasmid. A total of 365 random clones from the cosmid transformation of *M. smegmatis* were picked and grown in liquid medium (7H9) containing hygromycin (50 μg ml^{-1}). Assuming a random distribution of Mtb sequences among the cosmid transformants and an average insert size of ~40 kb, the 365 cosmid clones

represented approximately three times coverage (×*C*) of the entire Mtb genome (that is, ×*C* = *L*[*N*/*G*], where *L* is the average length of the genomic fragments represented by the inserts, *N* is the number of inserts, and *G* is the entire genome length). At this level of coverage, the probability of any given genomic 40 kb fragment being represented in a group of *N* cosmids is given by the formula $P = 1 - e^{-R}$, where $R = NL/G$ (ref. 49). For a library of 365 random cosmid clones, $P \cong 0.95$, indicating an approximately 95% chance that any given gene in Mtb will be assessed at least once in the initial screening. Cultures of BMDCs were infected at a multiplicity of infection (MOI) of 20:1 for 3 h individually with each of the 365 *M. smegmatis* clones containing Mtb cosmids. As a positive control, BMDCs were similarly infected with *M. smegmatis* expressing ESAT6-IEα and transformed with the empty pYUB412 cosmid vector. After 3 h, cells were treated with gentamicin (100 μg ml^{-1}; Invitrogen) for 1 h to inhibit the growth of extracellular bacteria and the cells were then washed two times with PBS and cultured in fresh medium containing 20 μg ml^{-1} of gentamicin. Cells were detached with cold PBS containing 1 mM EDTA at 24 h post-infection and were stained with the Y-Ae monoclonal antibody (specific for complexes of I-A^b/Eα peptide) and with mAbs specific for CD11c and for total MHC class II (I-A/I-E specific). Cell surface staining was measured by flow cytometry using a FACSCalibur (BD Biosciences). A total of 72 transformant clones of *M. smegmatis* showing significantly reduced Y-Ae staining (>3 standard errors below the mean value of 12 replicates of control clones containing an empty cosmid vector) were identified in primary screening. These were assessed for maintenance of expression of the ESAT6-IEα fusion protein by western blotting using anti-ESAT6 and anti-Hsp65 mAbs to assess the relative levels of the fusion protein with endogenous Hsp65 in each clone (see Supplementary Fig. 2a for an example). Eighteen of the 72 transformant clones initially selected by the primary screen (that is, 25%) showed reduced expression of the ESAT6-IEα fusion protein (ratio of Hsp65:ESAT6-IEα > 3 standard errors above values for empty cosmid control transformants) and these were excluded from subsequent secondary screening to eliminate false positives.

Cosmid recovery from *M. smegmatis*

Although pYUB412 is an integrating vector that inserts at a specific chromosomal site in *M. smegmatis*[50], we observed in preliminary studies that a small but significant amount of our integrated cosmids could be recovered by simple extraction from lysozyme-treated bacteria. This is due to a low rate of spontaneous excision and reinsertion of cosmids built in the pYUB412 backbone, which results in a constant low level of cells containing unintegrated circular cosmids. To recover these cosmids, *M. smegmatis* clones were grown in 250 ml of 7H9 medium at 37 °C overnight, collected by centrifugation, and resuspended in 4 ml of Glu TE buffer (50 mM glucose, 10 mM EDTA, 25 mM Tris, pH 7.5) with 10 mg ml^{-1} of lysozyme. The samples were incubated at 37 °C overnight. Then 40 ml of lysis buffer (1%SDS and 0.2 M NaOH) was added, mixed by inversion and incubated for 10 min on ice. After this, 40 ml of neutralization buffer (3 M potassium acetate, 2 M acetic acid) was added, mixed, and incubated for 10 min on ice. The samples were centrifuged and cleared by filtration through tissue paper to remove insoluble debris. Then 40 ml of 2-propanol was added to the supernatant, mixed and incubated for 10 min on ice, followed by centrifugation at 1,400*g* for 20 min. The pellets were recovered and resuspended in 4 ml of ultrapure water. A 4 ml volume of RNA precipitation buffer (5 M LiCl, 50 mM Tris, pH 7.6) was then added

and incubated for 10 min on ice. The samples were centrifuged for 10 min at 1,400*g*, and the supernatant was transferred to a new tube in which the DNA was precipitated by adding 80 μl of 10 M sodium acetate and 650 μl of ethanol, incubated at −20 °C for 20 min and then centrifuged. The pellets were washed twice with 70% ethanol, dried at room temperature and then resuspended in 100 μl of TE buffer.

DNA sequencing

The Mtb genomic DNA insert of each cosmid was first sequenced using primers specific for the sequences of the pYUB412 vector flanking the insert (pYB412F-5′-gtacgccaccgcctggttc-3′ and pYUB412R-5′-gtgccacctgacgtctaag-3′) which provided ~400 bp of Mtb genomic sequence corresponding to the 5′ and 3′ ends of the insert. Because initial analysis of the ends of the inserts revealed that they were composed of more than one fragment of genomic DNA that had been ligated in tandem, it was necessary to use a cosmid walking approach to obtain the complete sequences of the cosmid inserts. Sequencing by cosmid walking was done by starting from the distal portion of the known sequences at the ends of each insert. Deoxyoligonucleotides were designed based on the Mtb H37Rv genome sequence (http://genolist.pasteur.fr/TubercuList/) to be complementary to sequences located at 1 kbp intervals upstream of the known sequence and standard sequencing reactions were carried out using these as primers. Sequence information obtained from these reactions was used to design a second set of primers, and the process was repeated until all of the regions of the insert that were non-contiguous with the Mtb genomic sequence had been sequenced directly. This information was then used together with the published genomic sequence to assemble the complete insert sequence.

Animal experiments

Wild-type C57BL/6 or severe combined immunodeficiency (SCID; also in C57BL/6 background) female mice between six and eight weeks of age were purchased from Jackson Laboratories. Formal power calculations were not done for animal group size selection, although the minimum group size ($N = 5$) is typical for experiments to assess major effects on mycobacterial growth and virulence in the mouse infection model. This group size allows valid statistical testing in experiments with multiple groups. Animals were assigned randomly to experimental groups and studies using mice were not blinded. T cell receptor transgenic TEα mice (*rag1*−/−and expressing CD90.1) were a gift from Marc K. Jenkins (University of Minnesota). C57BL/6 mice were infected with Mtb or Δ*PE_PGRS47* or complemented strains through aerosol exposure as previously described[41]. SCID mice were infected i.v. via the tail vein with 1×10^6 c.f.u. per mouse. Lung tissues were processed for histopathology using standard paraffin fixation, sectioning and H&E staining. All mice were maintained under specific pathogen-free conditions. All procedures involving the use of animals were in compliance with protocols approved by the Albert Einstein College of Medicine Institutional Animal Use and Biosafety Committees.

Primary cell culture and cell lines

BMDCs were prepared as described[42]. Briefly, bone marrow was obtained from tibiae and femurs of six- to eight-week-old female C57BL/6 mice. Cells were seeded at 2×10^6 per 100 mm in bacteriological Petri dishes (VWR) in 10 ml of complete RPMI-1640 medium

(Invitrogen) supplemented with 10 mM HEPES, 2 mM L-glutamine, 55 μM 2-mercaptoethanol, 50 μg ml^{-1} penicillin/streptomycin and 10% ultralow IgG heat-inactivated (56 °C, 30 min) fetal bovine serum (FBS; Atlanta Biologicals) and murine granulocyte-macrophage colony-stimulating factor (GM-CSF) (20 ng ml^{-1}) (Peprotech). Cell cultures were fed with 10 ml of medium on days 3, 6 and 8 and collected on day 10. Bone marrow macrophages (BMMs) were derived according to previously published methods[43]. Briefly, marrow flushed from the tibia and femurs of six- to eight-week-old C57BL/6 mice was collected aseptically and cultured in non-tissue-culture-treated 100 × 20 mm serological plates (Fisher) at a density of 2×10^5 cells per ml in BMM medium (DMEM supplemented with 1% HEPES, 1% L-glutamine, 1% non-essential amino acids, 100 U ml^{-1} penicillin and 100 μg ml^{-1} streptomycin (all from Invitrogen), 10% FBS (HyClone/GE Healthcare) and 10% L929 fibroblast-conditioned medium) for 6 days. On day 6, adherent cells were collected after detachment by incubation for 20 min at 4 °C with 5 mM EDTA in PBS.

THP-1 cells (American Type Culture Collection (ATCC)) were grown in RPMI-1640 (Invitrogen) supplemented with 10% FBS, 1% HEPES, 1% non-essential amino acids and essential amino acids and 50 μg ml^{-1} of penicillin and streptomycin (complete RPMI). THP-1 cells were treated with 40 ng ml^{-1} phorbol ester (PMA; Sigma-Aldrich) overnight to induce their differentiation into macrophage-like cells. The J774 macrophage cell line (ATCC) was transduced to express a GFP-LC3 fusion protein using a lentivirus construct provided by N. Mizushima (Department of Physiology and Cell Biology, Tokyo Medical and Dental University)[44]. The J774-GFP-LC3, RAW 264.7 (ATCC) and AMJ2-C8 (ATCC) mouse macrophage lines were grown in DMEM supplemented with 1% HEPES, 1% l-glutamine, 1% non-essential amino acids, 100 U ml^{-1} penicillin, 100 μg ml^{-1} streptomycin (all from Invitrogen) and 10% FBS (HyClone). Immediately before infection with mycobacteria, these cells were washed and incubated with antibiotic-free media containing non-decomplemented FBS. Infections of cultured cells with mycobacteria were generally done for 3 h at 37 °C in a 5% CO_2 incubator, followed by washing three times with PBS and then culturing in fresh medium containing 100 μg ml^{-1} of gentamicin for 1 h. This was followed by washing and then incubation in media with gentamicin at 20 μg ml^{-1} for the additional indicated time periods. Approximately half of the culture medium was removed and replaced with fresh medium on day 3 of culture to improve viability through day 5.

The cell lines used in this study were authenticated and tested for mycoplasma at their source (ATCC) and were not tested subsequently for mycoplasma contamination.

Analysis of T-cell responses

To derive $CD4^+$ T-cell lines specific for the I-A^b presented Eα peptide, splenocytes from TEα transgenic mice were isolated by negative depletion (Pan T cell isolation kit, Miltenyi Biotech) and cultured with IEα peptide (10 μg ml^{-1}) in the presence of Gardiquimod (1 μg ml^{-1}) and poly I:C (10 μg ml^{-1}) for 7 days. The cells were then rested for an additional 7 days in the presence of irradiated syngeneic splenocytes, IL-2 (20 ng ml^{-1}) and IL-7 (10 ng ml^{-1}), after which they were again stimulated using IEα peptide plus irradiated splenocytes. After three cycles of restimulation followed by resting, the cells were collected and used for T-cell activation experiments.

Capture enzyme-linked immunosorbent assays (ELISA) for the detection of cytokines in supernatants of T-cell cultures were carried out as described previously[45]. Briefly, culture supernatants were collected after 72 h at 37 °C, and levels of IL-2 and IFNγ were quantified using specific capture and biotinylated detection mAb pairs (BD Biosciences), streptavidin-HRP (BD Biosciences) and TMB substrate (Sigma-Aldrich) as substrate. Recombinant cytokines (PeproTech) were used to generate standard curves. Measurements were performed in triplicate. Quantitation of IFNγ secreting $CD4^+$ T cells by ELISPOT was done as described previously[41], using synthetic peptides (10 μg ml^{-1}) corresponding to Mtb epitopes $Ag85B_{240–254}$ (Peptide 25), $ESAT6_{1–20}$ and $TB9.8_{46–61}$ for *in vitro* restimulation.

Fluorescence-activated cell sorting (FACS) analysis

Cells were suspended in FACS buffer (PBS, 2% FCS and 0.05% NaN_3) and Fc receptors were blocked by incubation for 5 min with a 1/10 dilution of a culture supernatant of the rat 2.4G2 hybridoma (specific for murine FcγRIII (CD16) and FcγRIIb (CD32)). Cells were stained with specific fluorochrome-labelled antibodies or peptide-loaded MHC class II tetramers in FACS buffer for 1 h at room temperature, washed twice and then resuspended in FACS buffer. Cells were analysed using a four-colour FACSCalibur cytometer (BD Biosciences).

Fluorescence microscopy and autophagy analysis

Autophagy was evaluated in infected cells by immunostaining of LC3 or by western blotting analysis as described previously[46]. For the quantification of autophagy, the percentages of GFP-LC3-positive autophagic vacuoles in J774 GFP-LC3 transfected cells, or the numbers of endogenous LC3 puncta in primary cells were evaluated using fluorescence microscopy. For immunostaining, macrophages with or without previous mycobacteria infection were seeded in wells of 24-well plates that contained round-glass coverslips at a density of $1×10^5$ cells per well in 1 ml of medium. For endogenous LC3 staining, cells were fixed with methanol at −20 °C for 20 min. For LAMP-1 staining, cells were fixed with 4% paraformaldehyde in PBS at 4 °C for 10 min and permeabilized with 0.01% Triton X-100 in PBS for 12 min before being treated with 10% bovine serum albumin (BSA) for 1 h at 25 °C. The cultures were then stained with primary antibodies, including rabbit anti-mouse LC3 (1:200; Cell Signaling) or rat anti-mouse LAMP-1 (1:200; Abcam) overnight at 4 °C. After washing to remove excess primary antibodies, the cultures were incubated for 2 h at room temperature with anti-rabbit IgG-Alexa 488 or anti-rat IgG-Alexa 647. In some experiments, RAW264.7 cells were loaded with Lysotracker DND RED (Life Technologies) and infected with different Mtb strains (wild type, Δ*PE_PGRS47* or complemented strain), which were fluorescently labelled with FITC (Sigma) for the indicated time periods and then washed three times with PBS before fixation for immunostaining. After washing, the sections were mounted with ProLong Gold (Invitrogen). Confocal images were acquired with a Leica SP5 AOBS (Leica Microsystems). Co-localization of fluorescent bacilli with lysosomal or autophagosomal markers was quantitated by direct visual scoring by a blinded observer, and by computer-assisted image analysis using ImageJ software (http://rsbweb.nih.gov/ij/). Criteria for the visual scoring were that positive scoring for co-localization had to satisfy two criteria: (1) the fluorescence from the marker being assessed had to surround more than half of the bacterial surface; and (2) the marker staining had to be

of sufficient intensity for the co-localized bacteria to appear distinctly yellow. In terms of quantitation, similar results were obtained using direct visual scoring and ImageJ analysis. The values of means ± s.e. of co-localization shown in Figs 2 and 3 were obtained with the direct visual scoring method. Endogenous LC3 conjugation was evaluated by western blot analysis using an antibody specific for LC3-I/II. As a positive control for autophagy activation, cells were treated with complete media contained 1 μM rapamycin (Sigma) for 12 h.

Electron microscopy

Transmission-electron microscopy was used to analyse the morphology of phagosomal membranes and to confirm the induction of autophagy. After infection with mycobacteria, cells were fixed with 2% glutaraldehyde in 0.1 M cacodylate at room temperature for 2 h and then incubated overnight in 4% formaldehyde, 1% glutaraldehyde and 0.1% PBS. After fixation, the samples were stained for 90 min in 2% osmium, then serially dehydrated in ethanol and embedded in Spurr's epoxy resin. Thin sections were obtained on an Ultracut cryotome and stained with 0.5% uranyl acetate and 0.5% lead citrate (Reichart). Samples were examined in a JEOL 1200EX transmission electron microscope operating at 80 kV. Immunogold electron microscopy was performed to analyse the presence of PE_PGRS protein after infection of macrophages with Msmeg or Msmeg-PE_PGRS47 using previously described methods[51]. Briefly, the macrophages were fixed in 0.1 M sodium cacodylate buffer (pH 7.2) containing 4% paraformaldehyde, 0.2% glutaraldehyde, infiltrated in 25% polyvinylpyrrolidone and 2.1 M sucrose and then rapidly frozen by immersion in liquid nitrogen. Cryosections were obtained in the temperature range from −70 to −90 °C using an Ultracut cryotome. After blocking with PBS–BSA with 50 mM NH_4Cl, the cryosections were incubated overnight in the presence of the mouse monoclonal antibody mAb 7C4.1F7. After incubation with Immunogold-labelled anti-mouse IgG, specimens were observed in a JEOL1200EX transmission electron microscope operating at 80 kV.

Supplementary Material

Refer to Web version on PubMed Central for supplementary material.

Acknowledgments

The authors thank the staff of the Flow Cytometry Core Facility of the Albert Einstein College of Medicine (supported by the Einstein Cancer Center grant NIH/NCI CA13330). The authors acknowledge the NIH Tetramer Core Facility (contract no. HHSN272201300006C) for provision of the I-A^b/TB9.8 tetramers. This work was supported by NIH grants AI093649 to S.A.P. and AI063537 to S.A.P., W.R.J. and J.C. The authors thank N. Mizushima, Tokyo Medical and Dental University, for providing the GFP-LC3 lentivirus construct and A.Y. Rudensky for providing the Y-Ae hybridoma. The authors also thank P. Jain and P. A. Gonzalez for their suggestions on the construction of the Δ*PE_PGRS47* mutant strain and R. Sellers for assistance in analysis of histopathology. A.B. acknowledges support from 'Estrategia de Sostenibilidad Universidad de Antioquia'. The authors thank R. Prados-Rosales for assistance with EM studies and E. Bejarano for advice on autophagy analysis.

References

1. Wolf AJ, et al. Mycobacterium tuberculosis infects dendritic cells with high frequency and impairs their function *in vivo*. J Immunol. 2007; 179:2509–2519. [PubMed: 17675513]

2. Mogues T, Goodrich ME, Ryan L, LaCourse R, North RJ. The relative importance of T cell subsets in immunity and immunopathology of airborne *Mycobacterium tuberculosis* infection in mice. J Exp Med. 2001; 193:271–280. [PubMed: 11157048]
3. Repique CJ, et al. Susceptibility of mice deficient in the MHC class II transactivator to infection with *Mycobacterium tuberculosis*. Scand J Immunol. 2003; 58:15–22. [PubMed: 12828554]
4. Scanga CA, et al. Depletion of $CD4^+$ T cells causes reactivation of murine persistent tuberculosis despite continued expression of interferon gamma and nitric oxide synthase 2. J Exp Med. 2000; 192:347–358. [PubMed: 10934223]
5. Baena A, Porcelli SA. Evasion and subversion of antigen presentation by *Mycobacterium tuberculosis*. Tissue Antigens. 2009; 74:189–204. [PubMed: 19563525]
6. Harding CV, Boom WH. Regulation of antigen presentation by *Mycobacterium tuberculosis*: a role for Toll-like receptors. Nature Rev Microbiol. 2010; 8:296–307. [PubMed: 20234378]
7. Pai RK, Convery M, Hamilton TA, Boom WH, Harding CV. Inhibition of IFN-γ-induced class II transactivator expression by a 19-kDa lipoprotein from *Mycobacterium tuberculosis*: a potential mechanism for immune evasion. J Immunol. 2003; 171:175–184. [PubMed: 12816996]
8. Pennini ME, et al. CCAAT/enhancer-binding protein β and δ binding to CIITA promoters is associated with the inhibition of CIITA expression in response to *Mycobacterium tuberculosis* 19-kDa lipoprotein. J Immunol. 2007; 179:6910–6918. [PubMed: 17982082]
9. Dengjel J, et al. Autophagy promotes MHC class II presentation of peptides from intracellular source proteins. Proc Natl Acad Sci USA. 2005; 102:7922–7927. [PubMed: 15894616]
10. Paludan C, et al. Endogenous MHC class II processing of a viral nuclear antigen after autophagy. Science. 2005; 307:593–596. [PubMed: 15591165]
11. Schmid D, Pypaert M, Munz C. Antigen-loading compartments for major histocompatibility complex class II molecules continuously receive input from autophagosomes. Immunity. 2007; 26:79–92. [PubMed: 17182262]
12. Zhou D, et al. Lamp-2a facilitates MHC class II presentation of cytoplasmic antigens. Immunity. 2005; 22:571–581. [PubMed: 15894275]
13. Singh SB, Davis AS, Taylor GA, Deretic V. Human IRGM induces autophagy to eliminate intracellular mycobacteria. Science. 2006; 313:1438–1441. [PubMed: 16888103]
14. Gutierrez MG, et al. Autophagy is a defense mechanism inhibiting BCG and *Mycobacterium tuberculosis* survival in infected macrophages. Cell. 2004; 119:753–766. [PubMed: 15607973]
15. Shin DM, et al. Mycobacterium tuberculosis Eis regulates autophagy, inflammation, and cell death through redox-dependent signaling. PLoS Pathogens. 2010; 6:e1001230. [PubMed: 21187903]
16. Romagnoli A, et al. ESX-1 dependent impairment of autophagic flux by *Mycobacterium tuberculosis* in human dendritic cells. Autophagy. 2012; 8:1357–1370. [PubMed: 22885411]
17. Espert L, Beaumelle B, Vergne I. Autophagy in *Mycobacterium tuberculosis* and HIV infections. Front Cell Infect Microbiol. 2015; 5:49. [PubMed: 26082897]
18. Rudensky A, Preston-Hurlburt P, Hong SC, Barlow A, Janeway CA Jr. Sequence analysis of peptides bound to MHC class II molecules. Nature. 1991; 353:622–627. [PubMed: 1656276]
19. Deretic V, Saitoh T, Akira S. Autophagy in infection, inflammation and immunity. Nature Rev Immunol. 2013; 13:722–737. [PubMed: 24064518]
20. Munz C. Enhancing immunity through autophagy. Annu Rev Immunol. 2009; 27:423–449. [PubMed: 19105657]
21. Mizushima N, Yoshimori T, Levine B. Methods in mammalian autophagy research. Cell. 2010; 140:313–326. [PubMed: 20144757]
22. Tian C, Jian-Ping X. Roles of PE_PGRS family in *Mycobacterium tuberculosis* pathogenesis and novel measures against tuberculosis. Microb Pathog. 2010; 49:311–314. [PubMed: 20638467]
23. Brennan MJ, Delogu G. The PE multigene family: a 'molecular mantra' for mycobacteria. Trends Microbiol. 2002; 10:246–249. [PubMed: 11973159]
24. Bardarov S, et al. Specialized transduction: an efficient method for generating marked and unmarked targeted gene disruptions in *Mycobacterium tuberculosis*, *M bovis* BCG and *M smegmatis*. Microbiology. 2002; 148:3007–3017. [PubMed: 12368434]

25. Rusten TE, Stenmark H. p62, an autophagy hero or culprit? Nature Cell Biol. 2010; 12:207–209. [PubMed: 20190829]
26. Bold TD, Banaei N, Wolf AJ, Ernst JD. Suboptimal activation of antigen-specific CD4$^+$ effector cells enables persistence of *M. tuberculosis in vivo*. PLoS Pathogens. 2011; 7:e1002063. [PubMed: 21637811]
27. Reiley WW, et al. ESAT-6-specific CD4T cell responses to aerosol *Mycobacterium tuberculosis* infection are initiated in the mediastinal lymph nodes. Proc Natl Acad Sci USA. 2008; 105:10961–10966. [PubMed: 18667699]
28. Kruh NA, Troudt J, Izzo A, Prenni J, Dobos KM. Portrait of a pathogen: the *Mycobacterium tuberculosis* proteome *in vivo*. PLoS ONE. 2010; 5:e13938. [PubMed: 21085642]
29. Simeone R, Bottai D, Frigui W, Majlessi L, Brosch R. ESX/type VII secretion systems of mycobacteria: insights into evolution, pathogenicity and protection. Tuberculosis (Edinb). 2015; 95(Suppl 1):S150–S154. [PubMed: 25732627]
30. Srivastava V, Jain A, Srivastava BS, Srivastava R. Selection of genes of *Mycobacterium tuberculosis* upregulated during residence in lungs of infected mice. Tuberculosis (Edinb). 2008; 88:171–177. [PubMed: 18054522]
31. Copin R, et al. Sequence diversity in the pe_pgrs genes of *Mycobacterium tuberculosis* is independent of human T cell recognition. mBio. 2014; 5:e00960–e00913. [PubMed: 24425732]
32. Lee HK, et al. In vivo requirement for Atg5 in antigen presentation by dendritic cells. Immunity. 2010; 32:227–239. [PubMed: 20171125]
33. Deretic V. Autophagy, an immunologic magic bullet: *Mycobacterium tuberculosis* phagosome maturation block and how to bypass it. Future Microbiol. 2008; 3:517–524. [PubMed: 18811236]
34. Koul A, Herget T, Klebl B, Ullrich A. Interplay between mycobacteria and host signalling pathways. Nature Rev Microbiol. 2004; 2:189–202. [PubMed: 15083155]
35. Watson RO, Manzanillo PS, Cox JS. Extracellular *M tuberculosis* DNA targets bacteria for autophagy by activating the host DNA-sensing pathway. Cell. 2012; 150:803–815. [PubMed: 22901810]
36. Ouimet M, et al. Mycobacterium tuberculosis induces the miR-33 locus to reprogram autophagy and host lipid metabolism. Nature Immunol. 2016; 17:677–686. [PubMed: 27089382]
37. Kimmey JM, et al. Unique role for ATG5 in neutrophil-mediated immunopathology during *M tuberculosis* infection. Nature. 2015; 528:565–569. [PubMed: 26649827]
38. Cadieux N, et al. Induction of cell death after localization to the host cell mitochondria by the *Mycobacterium tuberculosis* PE_PGRS33 protein. Microbiology. 2011; 157:793–804. [PubMed: 21081760]
39. Braunstein M, Bardarov SS, Jacobs WR Jr. Genetic methods for deciphering virulence determinants of *Mycobacterium tuberculosis*. Methods Enzymol. 2002; 358:67–99. [PubMed: 12474379]
40. Stover CK, et al. New use of BCG for recombinant vaccines. Nature. 1991; 351:456–460. [PubMed: 1904554]
41. Hinchey J, et al. Enhanced priming of adaptive immunity by a proapoptotic mutant of *Mycobacterium tuberculosis*. J Clin Invest. 2007; 117:2279–2288. [PubMed: 17671656]
42. Lutz MB, et al. An advanced culture method for generating large quantities of highly pure dendritic cells from mouse bone marrow. J Immunol Methods. 1999; 223:77–92. [PubMed: 10037236]
43. Houben EN, Nguyen L, Pieters J. Interaction of pathogenic mycobacteria with the host immune system. Curr Opin Microbiol. 2006; 9:76–85. [PubMed: 16406837]
44. Mizushima N, Yamamoto A, Matsui M, Yoshimori T, Ohsumi Y. *In vivo* analysis of autophagy in response to nutrient starvation using transgenic mice expressing a fluorescent autophagosome marker. Mol Biol Cell. 2004; 15:1101–1111. [PubMed: 14699058]
45. Forestier C, et al. Improved outcomes in NOD mice treated with a novel Th2 cytokine-biasing NKT cell activator. J Immunol. 2007; 178:1415–1425. [PubMed: 17237389]
46. Yuk JM, et al. Vitamin D3 induces autophagy in human monocytes/macrophages via cathelicidin. Cell Host Microbe. 2009; 6:231–243. [PubMed: 19748465]

47. Averill LE, et al. Screening of a cosmid library of *Mycobacterium bovis* BCG in *Mycobacterium smegmatis* for novel T-cell stimulatory antigens. Res Microbiol. 1993; 144:349–362. [PubMed: 8248628]

48. Barlow AK, He X, Janeway C Jr. Exogenously provided peptides of a self-antigen can be processed into forms that are recognized by self-T cells. J Exp Med. 1998; 187:1403–1415. [PubMed: 9565633]

49. Clarke L, Carbon J. A colony bank containing synthetic Col El hybrid plasmids representative of the entire *E. coli* genome. Cell. 1976; 9:91–99. [PubMed: 788919]

50. Pavelka MS Jr, Jacobs WR Jr. Comparison of the construction of unmarked deletion mutations in *Mycobacterium smegmatis Mycobacterium bovis* bacillus Calmette-Guerin, and *Mycobacterium tuberculosis* H37Rv by allelic exchange. J Bacteriol. 1999; 181:4780–4789. [PubMed: 10438745]

51. Prados-Rosales R, et al. Mycobacteria release active membrane vesicles that modulate immune responses in a TLR2-dependent manner in mice. J Clin Invest. 2011; 121:1471–1483. [PubMed: 21364279]

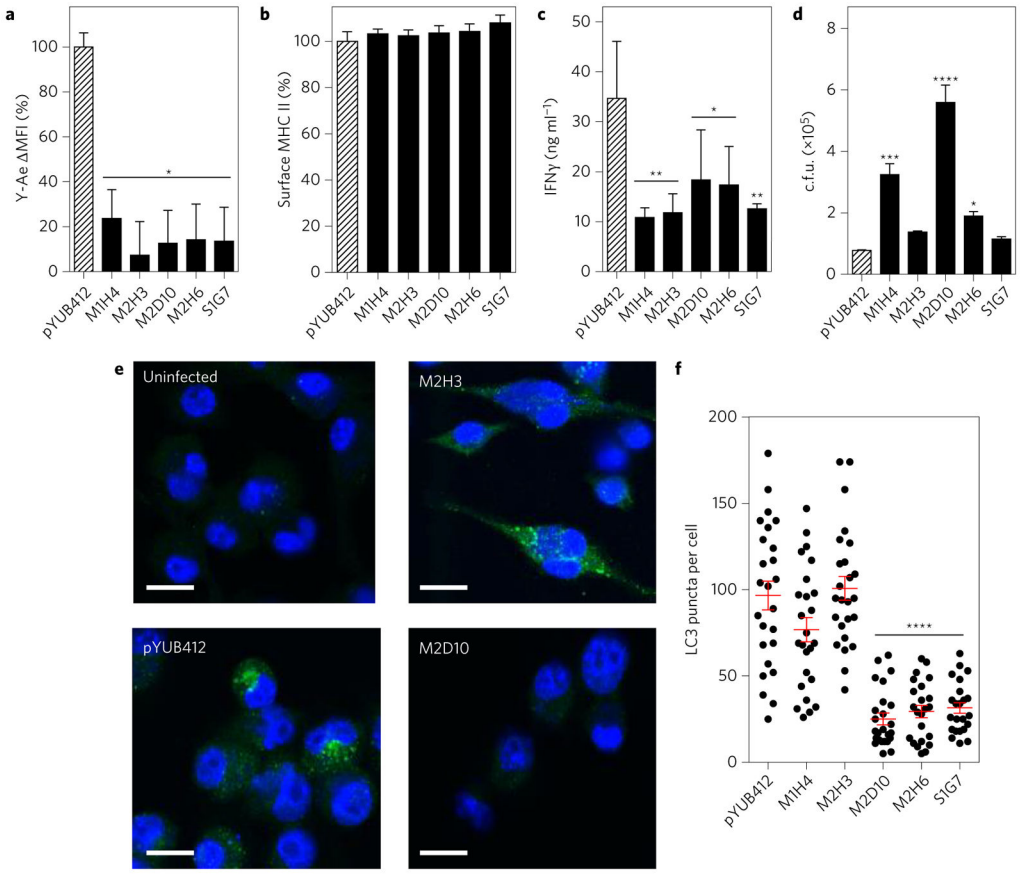

Figure 1. Identification of Mtb cosmid clones that inhibit MHC class II antigen presentation

a, BMDCs were infected at a multiplicity of infection (MOI) of 20:1 for 3 h with Msmeg expressing ESAT6-IEα and either the Mtb genomic cosmid clones indicated (filled bars) or an empty cosmid (pYUB412, hatched bar). Cells were collected 24 h after infection, stained with mAb Y-Ae and analysed by flow cytometry. The increase in mean fluorescence intensity (MFI) compared to the background level of BMDCs infected with Msmeg not expressing ESAT6-IEα was determined (ΔMFI). All ΔMFI values are plotted as a percentage of the value for the pYUB412 control, which was normalized to 100. **b**, BMDCs were infected as in **a**, but stained with mAb specific for total MHC class II. Values are plotted as MFI of surface staining as a percentage of the pYUB412 control (hatched bar), which was normalized to 100. **c**, Cells from a Th1-polarized $CD4^+$ T-cell line derived from TEα TCR transgenic mice were cultured with BMDCs infected as outlined in **a**. Supernatants were collected after 72 h and the levels of IFNγ were measured by capture ELISA. **d**, BMDCs were infected as in **a**. Cells were collected after 24 h of incubation and lysates were plated to determine the number of intracellular viable bacteria. **e**, Fluorescence images of AMJ2-C8 infected as in **a** and immunostained with anti-LC3 and with DAPI after a total of 24 h. Representative images of cells uninfected or infected with Msmeg transformed with empty cosmid (pYUB412), or with cosmids M2H3 or M2D10 (green, LC3; blue, DAPI). Scale bars, 20 μm. **f**, Quantitative analysis of the percentages of $LC3^+$ punctate foci per cell for all five cosmids. $*P < 0.05$, $**P < 0.01$, $***P < 0.001$, $****P <$

0.0001 compared to control (pYUB412) values (one-way analysis of variance (ANOVA) with Dunnett's multiple comparisons post-test). All values are plotted as means ± 1 s.e. of triplicate measurements and the results are representative of a minimum of three independent experiments (**a**–**d**) and two independent experiments (**e**,**f**). Means and s.e. are indicated in red.

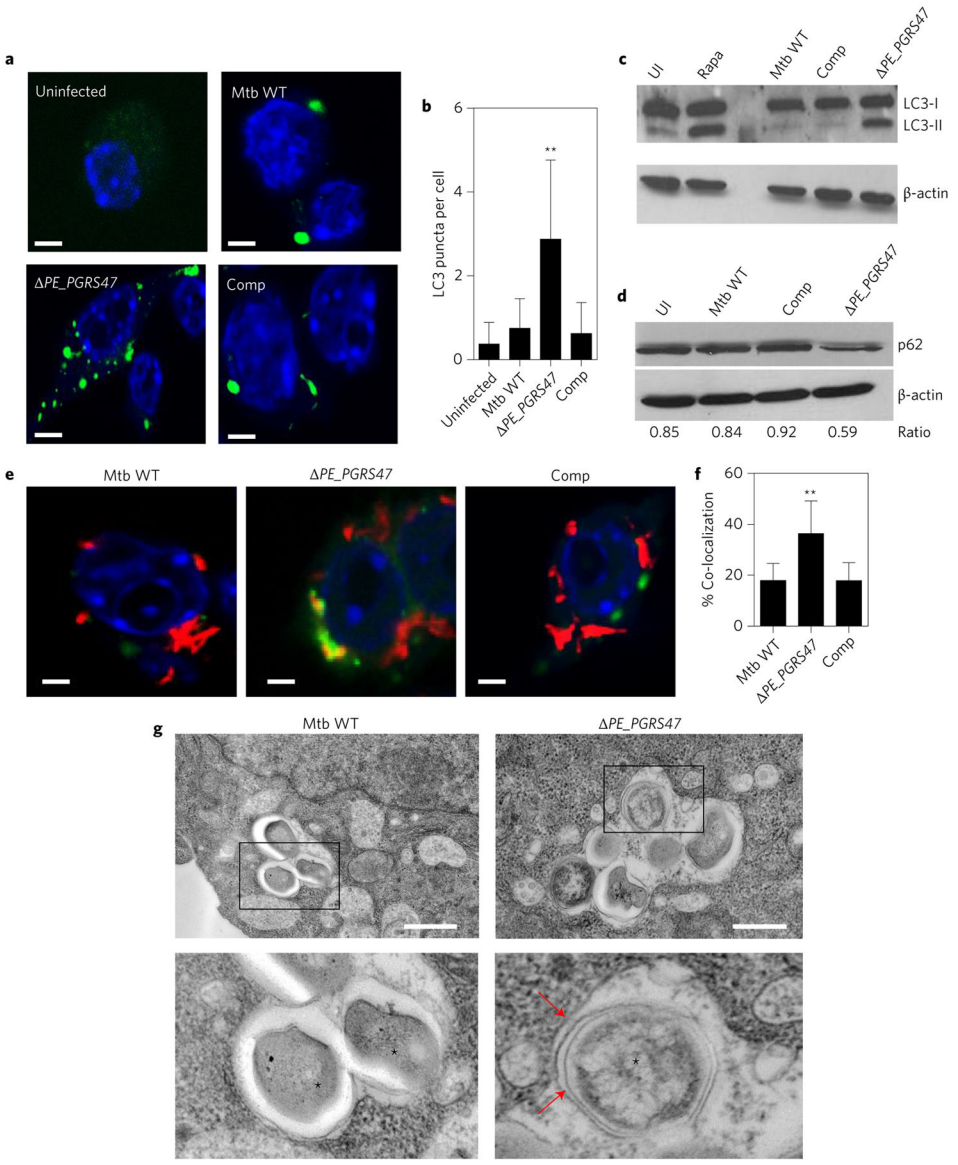

Figure 2. Inhibition of autophagy by *PE_PGRS47*

a, Fluorescence images of RAW 264.7 macrophages infected with indicated Mtb strains at an MOI of 20:1 for 3 h and immunostained with anti-LC3 and with DAPI after a total of 24 h. Representative images from one of three independent experiments are shown. Scale bars, 5 μm. **b**, Quantification of $LC3^{+}$ puncta per cell, showing means ± 1 s.e. of triplicate cultures analysed in blinded fashion. $^{**}P < 0.01$ compared to cells infected with Mtb WT (one-way ANOVA with Dunnett's post-test). **c**, RAW 264.7 cells were infected as in **a** and incubated for an additional 20 h or left uninfected (UI) or treated for the final 12 h with 1 μM rapamycin (Rapa). Cells were collected and subjected to western blot analysis for LC3-I and LC3-II, and for β-actin as a loading control. **d**, RAW 264.7 cells were infected and incubated as in **c** and analysed by western blot for p62 (SQSTM1) or for β-actin as a loading control. The ratio of the intensities of the p62 to β-actin bands is indicated below each lane. **e**, Merged fluorescence images of RAW 264.7 cells infected with the indicated strains of

Mtb expressing TdTomato (red) for 3 h at an MOI of 20:1 and immunostained with anti-LC3 (green) and with DAPI (blue) after a total of 24 h of incubation. Co-localization of red (bacteria) with green (LC3) signals is indicated in yellow. Scale bars, 5 μm. **f**, Quantitation of co-localization (percentage of red bacteria also stained green) observed in **e**. Mean values ± 1 s.e. are plotted for ~100 cells for each condition analysed in blinded fashion. $^{**}P < 0.01$ versus Mtb wild type (WT) infected (one-way ANOVA with Dunnett's post-test). **g**, Transmission electron micrographs of RAW 264.7 cells infected as in **a** and collected after 24 h of incubation. A representative field is shown for each condition and the areas within the black boxes are enlarged below. Asterisks mark intracellular bacilli, and red arrows indicate double membrane structures consistent with newly formed autophagosomes. Scale bars, 0.5 μm. Results shown are representative of three independent experiments (**a**–**f**) or two independent experiments (**g**).

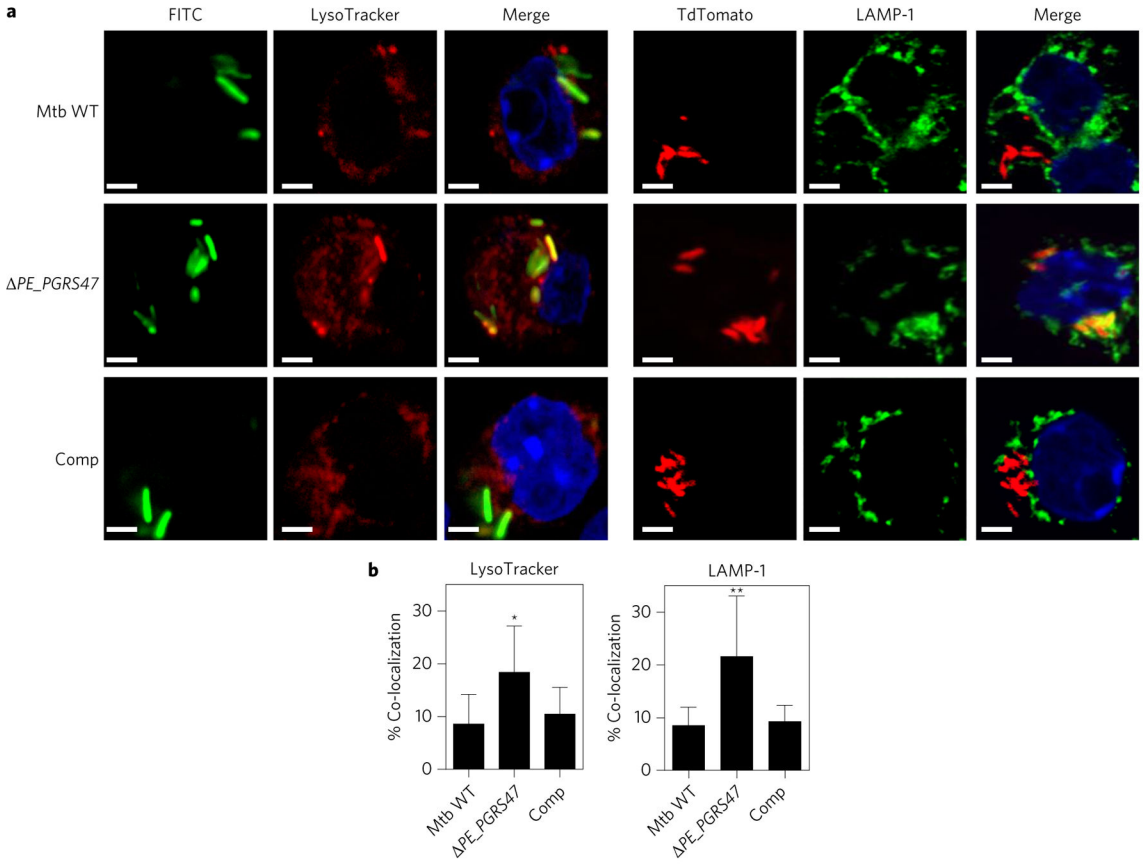

Figure 3. Increased acidification and lysosomal fusion of phagosomes containing Mtb Δ*PE_PGRS47*

a, Macrophages (RAW 264.7 cells) were infected with wild-type Mtb (Mtb WT), Δ*PE_PGRS47* or complemented (Comp) strains that were either FITC labelled (left) or expressing TdTomato (right) using an MOI of 20:1 for 3 h followed by gentamicin (100 μg ml^{-1}) treatment for 1 h, and then incubated for an additional 20 h. Cells were either stained with LysoTracker DND Red (red, left) before fixation, or fixed and permeabilized and stained with monoclonal LAMP-1 antibody (green, right). DAPI was used to stain nuclei (blue). Cells were analysed by confocal immunofluorescence microscopy and representative images are shown with yellow representing co-localization of red and green fluorescent signals. Scale bars, 5 μm. **b**, Quantitation of co-localization of bacteria with LysoTracker DND Red or LAMP-1. Mean values ± 1 s.e. are plotted for the percentage of bacteria co-localizing with LysoTracker signal or LAMP-1 in ~100 random cells analysed in blinded fashion. *$P < 0.05$, **$P < 0.01$ for Mtb WT versus Δ*PE_PGRS47* (one-way ANOVA with Dunnett's post-test).

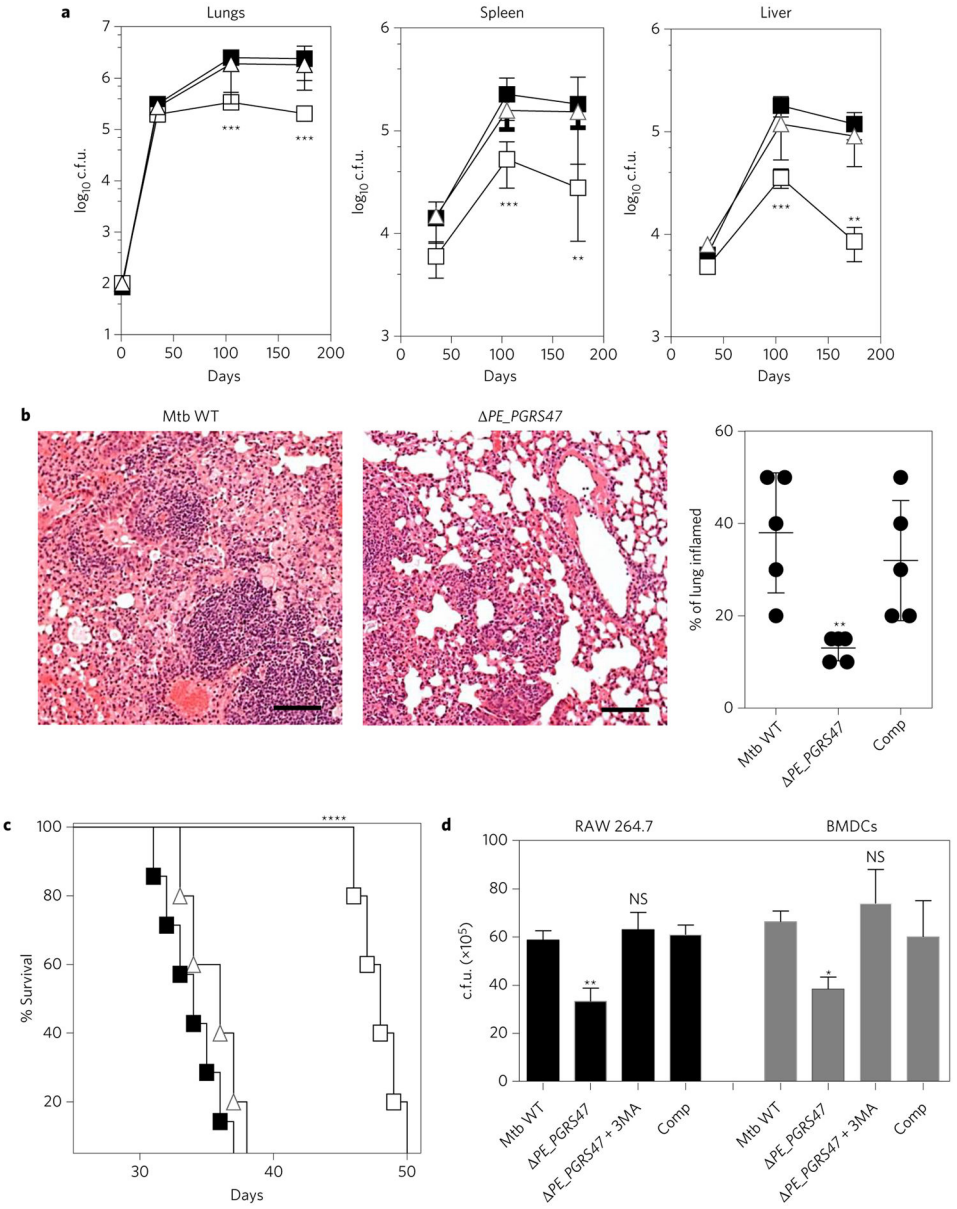

Figure 4. *PE_PGRS47* is required for full virulence at late stages of Mtb infection

a, Bacterial load in the lungs, spleens and livers of C57BL/6 mice infected with low- dose aerosol (~100 c.f.u.) of WT Mtb (filled squares), Δ*PE_PGRS47* mutant (open squares) or complemented (open triangles) strains. Values shown are means ± 1 s.d. for five mice per time point. $^{**}P < 0.01$, $^{***}P < 0.001$ for mutant compared to WT Mtb infected (two-way ANOVA with Dunnett's post-test). The results shown are representative of two experiments. **b**, Representative H&E-stained lung sections are shown for C57BL/6 mice at 15 weeks post-infection with low-dose aerosol (~100 c.f.u.) of WT Mtb or Δ*PE_PGRS47* mutant. Scale bars, 200 μm. The graph on the right shows quantification of the estimated percentage of total lung tissue affected by inflammation and cellular infiltrates, based on visual scoring of lung sections from individual mice ($N = 5$ per group) carried out in blinded fashion. Means are indicated by horizontal lines and error bars show ± 1 s.e. $^{**}P < 0.05$ compared to Mtb

infected (two-way ANOVA with Dunnett's post-test). This analysis was performed once. **c**, Survival of SCID mice ($n = 7$) infected intravenously with 1×10^6 c.f.u. per mouse of WT Mtb (filled square), Δ*PE_PGRS47* mutant (open squares) or complemented (open triangles) strains. ****$P < 0.0001$ (log rank test). This experiment was performed once. **d**, RAW 264.7 cells (black) or BMDCs (grey) were infected with WT Mtb (Mtb WT), Δ*PE_PGRS47* or complemented (Comp) strains using an MOI of 10:1 for 3 h followed by gentamicin (100 μg ml^{-1}) treatment for 1 h. Cultures were incubated for an additional 20 h and then collected, lysed and plated to determine c.f.u. of viable bacteria. Where indicated, 3-methyladenine (3MA, 5 mM) was added 1 h before infection. This experiment was performed twice and representative results are shown. *$P < 0.05$, **$P < 0.01$ for Mtb WT versus Δ*PE_PGRS47* (one-way ANOVA with Dunnett's post-test). NS, not significant.

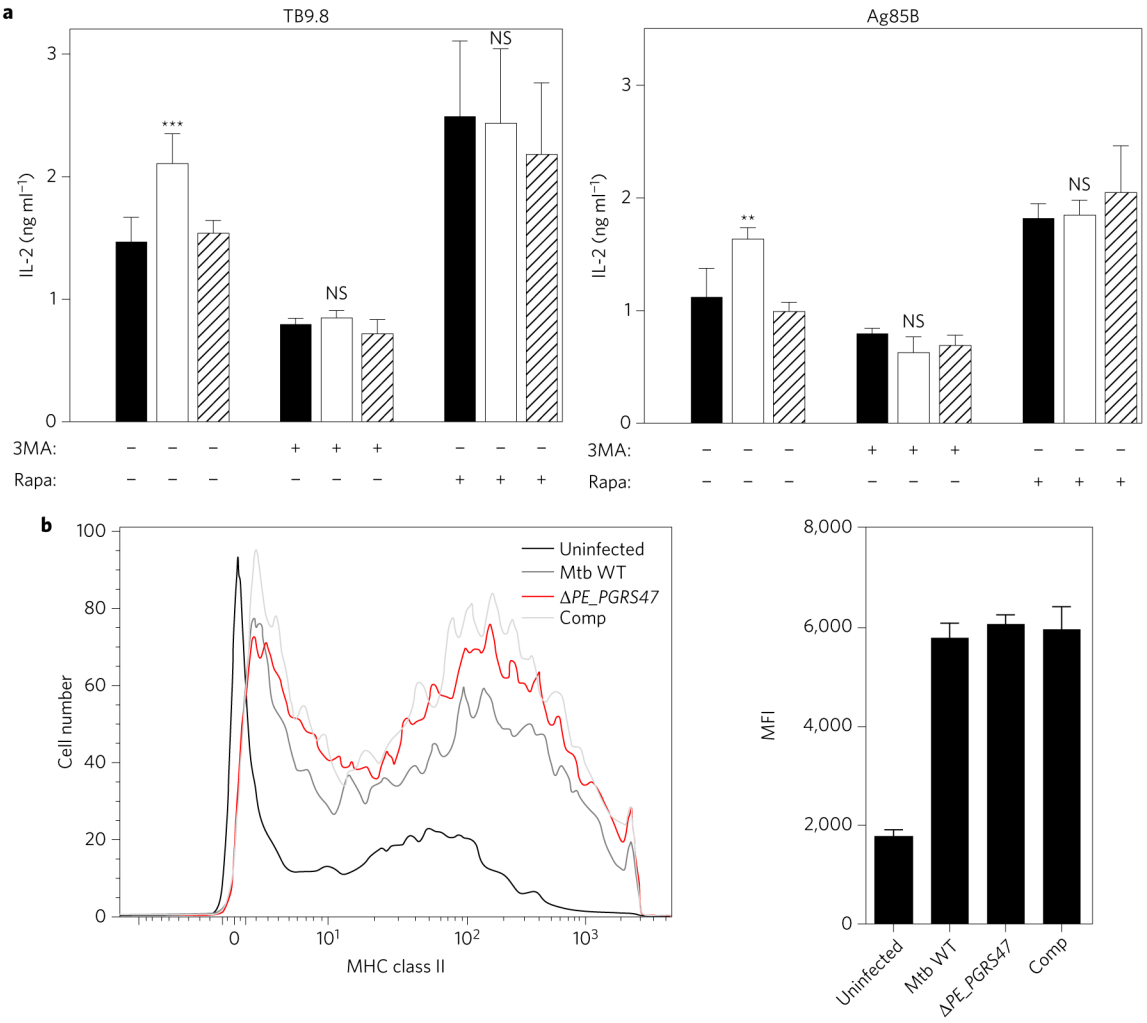

Figure 5. Autophagy-dependent enhancement of MHC class II antigen presentation during *in vitro* infection by the Mtb ΔPE_PGRS47 mutant

a, IL-2 concentrations in supernatants from co-cultures of Mtb antigen-specific T-cell hybridomas and BMDCs infected with wild-type (solid bars), ΔPE_PGRS47 mutant (open bars) or complemented (hatched bars) strains of Mtb. Infection was with an MOI of 10:1 for 3 h followed by gentamicin (100 μg ml^{-1}) treatment for 1 h and then incubation with TB9.8-specific (left) or Ag85B-specific (right) T-cell hybridomas for an additonal 20 h. Rapamycin (Rapa, 1 mM) or 3-methyladenine (3MA, 5 mM) was added to some cultures as indicated 1 h before infection. Concentrations of IL-2 were determined from triplicate wells by ELISA and values are plotted as means ± 1 s.e. Background levels of IL-2 in cultures with no mycobacterial infection were <0.1 ng ml^{-1} for both T-cell hybridomas. Asterisks indicate significant differences compared to WT Mtb (** $P < 0.01$ and *** $P < 0.001$); NS, not significant compared to Mtb WT (two-way ANOVA with Dunnett's post-test). **b**, Lack of effect of PE_PGRS47 expression on surface MHC class II levels of infected BMDCs. Cultures of BMDCs were infected with the indicated bacteria at an MOI of 10:1 for 3 h followed by gentamicin (100 μg ml^{-1}) treatment for 1 h and then incubated for an additional 20 h. Cells were then surface-stained with anti-CD11c-PE and anti-MHC class II-APC

conjugates and analysed by flow cytometry. Representative histograms are shown for MHC class II staining on cells gated for CD11c expression (left) and the bar graph (right) shows the average of mean fluorescence intensity (MFI) ± 1 s.e. for triplicate cultures either uninfected or infected with the indicated Mtb WT, Δ*PE_PGRS47* mutant (Δ*PE_PGRS47*) or complemented (Comp) strains. Results shown in **a** and **b** are representative of two independent experiments.

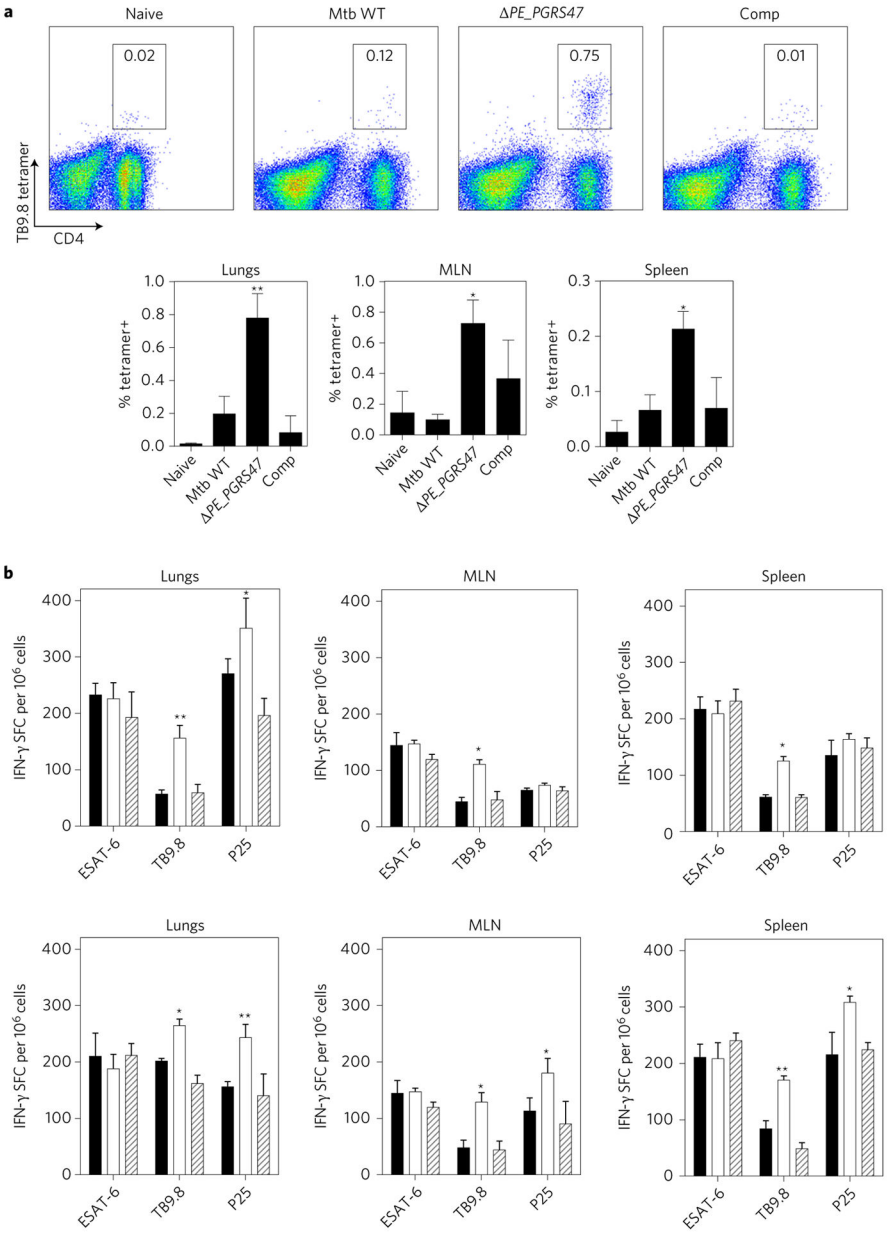

Figure 6. Suppression of CD4$^+$ T-cell responses by *PE_PGRS47*

a, C57BL/6 mice (n = 5 per group) were infected with low-dose aerosol (~100 c.f.u.) of wild-type Mtb, Δ*PE_PGRS47* mutant or complemented strains. Lungs, mediastinal lymph nodes (MLNs) and spleens were collected on day 24, and cells from each tissue were pooled for each group. Five samples from each pool were then stained with anti-CD4 mAb and MHC class II (I-A^b) tetramers loaded with TB9.8 peptide. Dot plots (top) show representative examples of flow cytometry analysis for TB9.8 tetramer positive cells in the lungs of either uninfected control mice (naive), or mice infected with the indicated Mtb strains. Rectangular regions enclose tetramer-positive cells and frequencies as a percentage of total CD4$^+$ cells are shown. Bar graphs (bottom) show mean values ± 1 s.e. for tetramer positive cells in each tissue for five replicate samples from the pooled cells of each group of

five mice. *$P < 0.05$, **$P < 0.01$ for mutant (Δ*PE_PGRS47*) versus Mtb WT infected (one-way ANOVA with Dunnett's post-test). **b**, C57BL/6 mice ($n = 5$) were infected as in **a** with WT Mtb (black bars), Δ*PE_PGRS47* (open bars) or complemented (hatched bars) strains. Lungs, MLNs and spleens were collected on day 24 (top) or day 60 (bottom) post-infection. Single-cell suspensions were prepared and cells from each tissue were pooled for each group. $CD4^+$ T cells were purified and ELISPOT was used to detect IFNγ-spot forming cells (SFC) responding to re-stimulation *in vitro* with Mtb peptides corresponding to $I\text{-}A^b$ presented epitopes of Mtb antigens ESAT-6, TB9.8 and Ag85B (P25). Each bar represents means ± 1 s.e. of four replicate ELISPOT wells. *$P < 0.05$, **$P < 0.01$ for comparisons of Δ*PE_PGRS47* versus WT Mtb (one-way ANOVA with Dunnett's post-test). Results shown in **a** and **b** are representative of two similar experiments.